RSC Advances

PAPER

View Article Online
View Journal | View Issue

Cite this: *RSC Adv.*, 2021, **11**, 23968

Influence of amphiphilic molecules on the peroxidase-like behavior of nanoparticles in an aqueous solution

Tianxiang Yin, †*[a] Xingnan Zhou†[b] and Jing Shi[a]

Received 29th April 2021
Accepted 23rd June 2021

DOI: 10.1039/d1ra03345j

rsc.li/rsc-advances

Carbon dots (CDs) have drawn considerable attention in recent decades due to their outstanding biocompatibility and environmental friendliness. In this study, we synthesized ionic liquid (1-aminopropyl-3-methyl-imidazolium bromide)-modified carbon dots (IL-CDs) showing good peroxidase-like activity. Furthermore, we investigated their enzymic behavior in the presence of two different amphiphilic molecules, namely *tert*-butanol (TBA, a typical hydrotrope) and sodium bis (2-ethylhexyl) sulfosuccinate (AOT, a typical anionic surfactant). In an aqueous solution of TBA, a microscopic heterogeneous structure was formed in a certain concentration range of TBA, which resulted in an anomaly in the reaction process. However, in the AOT aqueous solution, the situation became more complicated. IL-CDs formed vesicles or precipitation at different concentrations of AOT, which led to different enzymic activities of IL-CDs due to the variance in the structure and the surface electronic density.

1. Introduction

In recent years, nanomaterials showing enzyme-like activity have attracted wide attention after the pioneer study by Yan *et al.*[1] due to their simple preparation process, low cost, tunable catalytic activity and high stability, *etc.*, which avoid the high requirements on reaction conditions for the use of natural peroxidase and serve as a new generation of artificial enzymes. Different types of nanomaterials, including Fe_3O_4, MnO_2, and noble nanoparticles, have been reported and shown potential application in various fields.[2,3]

Since the accidental discovery of carbon dots (CDs) in 2004,[4] their unique nature and potential applications have quickly attracted the interest of researchers in different fields.[5,6] Recently, different types of CDs as well as corresponding hybrid materials have been reported to exhibit peroxidase-like activity[7–11] at relatively high temperature and wide pH range. When applying these materials in practice, the systems may be more complicated and different kinds of molecules may exist, which may result in different structures in solution. Amphiphilic molecules such as surfactants and hydrotropes are widely used to enhance the solubility of hydrophobic substances. Surfactants can form numerous types of aggregate structures at certain concentrations. However, hydrotropes may not result in these typical aggregates, but can induce the formation of a meso-scale structure in the solution under appropriate conditions and influence the chemical reactions performed in hydrotrope solutions.[12,13] However, research concerning the effects of solution structures on the enzymic activity of nano-enzymes have rarely been reported.

In this study, positively charged and ionic liquid-modified carbon dots (IL-CDs) were synthesized by a hydrothermal method. The morphology and surface structure were characterized. Moreover, the peroxidase-like activities of the IL-CDs were investigated by the catalytic oxidation of 3,3′,5,5′-tetramethylbenzidine (TMB) in the presence of H_2O_2 both in water and in the presence of different types of amphiphilic molecules, such as *tert*-butanol and sodium bis(2-ethylhexyl)sulfosuccinate (AOT). Different behaviors of IL-CDs in aqueous solutions of TBA and AOT were observed and discussed, which provided deep insight into the application of nano-enzymes.

2. Experimental section

2.1 Materials

1-Aminopropyl-3-methyl-imidazolium bromide ([APMIm][Br], ≥99 wt%) was obtained from Lanzhou Institute of Chemical Physics, Chinese Academy of Sciences (China). Citric acid monohydrate (CA, ≥99.5 wt%), thiourea (≥99 wt%), potassium dihydrogen phosphate (≥99 wt%) and disodium hydrogen phosphate (≥99 wt%) were purchased from Shanghai Runjie Chemical Reagent Co., Ltd. Sodium bis(2-ethylhexyl) sulfosuccinate (AOT, >99% wt%) was purchased from Sigma-Aldrich Chemical Co. 3,3′,5,5′-Tetramethylbenzidine (TMB, 98 wt%), ethanol (99 wt%), and *tert*-butanol (TBA, 99 wt%) were supplied

[a]*School of Chemistry and Molecular Engineering, East China University of Science and Technology, Shanghai 200237, China. E-mail: yintx@ecust.edu.cn; Fax: +86 21 64250804; Tel: +86 21 64252012*

[b]*The Affiliated Huai'an Hospital of Xuzhou Medical University and the Second People's Hospital of Huai'an, Huai'an 223002, China*

† These two authors contributed equally to this work.

by Aladdin. Hydrogen peroxide (H_2O_2, 30 wt%) was obtained from Chinasun Specialty Products Co., Ltd All reagents were used directly without further purification, and all aqueous solutions were prepared with ultrapure water (18.2 MΩ) from a ultra-pure water system (DZG-303A, Leading Water Treatment Co. Ltd, Shanghai).

2.2 Preparation of ionic liquid modified carbon dots (IL-CDs)

IL-CDs were prepared by a method that is similar to that reported by Shi *et al.*[8] and Wang *et al.*[14] In brief, citric acid monohydrate (0.63 g), thiourea (0.171 g) and [APMIm][Br] (1.76 g) were added to a round-bottom flask containing 15 ml water under vigorous stirring until the mixture was totally dissolved. The mixture was then transferred to a hydrothermal autoclave and heated to 180 °C using an oil bath, followed by a pyrolization process at 180 °C for 2 h. After cooling naturally to room temperature, the mixture was re-dispersed in water and further dialyzed against water for 72 h using a dialysis bag (1000 Da) to remove unreacted small molecules. The obtained transparent IL-CD solution was stored at 4 °C for further use.

2.3 Characterizations of IL-CDs

The high-resolution transmission electron microscopy (HRTEM) images of IL-CDs in both absence and presence of TBA were recorded using a JEOL-2010 electron microscope (Japan) operating at 200 kV. For negative-staining transmission electron microscopy (NS-TEM) observations, samples were placed on a carbon-coated copper grid and then stained with 1% uranyl acetate, and further observed on a JEM-100 CXII electron microscope (JEOL, Japan) at an accelerating voltage of 120 kV. UV-vis absorption spectra of the obtained IL-CDs were recorded on a UV-vis spectrophotometer (UV-2450, Shimadzu, Japan). The Fourier transform infrared (FT-IR) spectra of IL-CDs were recorded in the range of 500–4000 cm^{-1} using a NICOLET iS10 (Thermo Fisher, America) spectrometer. The X-ray diffraction (XRD) measurements of IL-CDs were performed on a Rotating Anode X-ray Powder Diffractometer (D/max-2550VB/PC, Rigaku) in the absence and presence of AOT. The X-ray photoelectron spectra (XPS) of the IL-CDs were performed on an ESCALAB 250 spectrometer (Thermo Fisher, America). Zeta potential of IL-CDs in solutions with and without the presence of AOT was measured to show the surface charge by a Malvern Zetasizer NanoZS instrument (Southborough, MA) equipped with a laser Doppler velocimeter using a folded capillary cell with a gold electrode.

2.4 Peroxidase-like activities of IL-CDs

The peroxidase-like activities of the as-synthesized IL-CDs were investigated by the catalytic oxidation of a chromogenic substrate (TMB) in the presence of H_2O_2. Typically, in the absence of amphiphilic molecules, a certain amount of TMB, H_2O_2, and the IL-CD solution were mixed in a citrate–phosphate (0.2 M) buffer solution at a certain pH and temperature. The reaction was monitored by automatically recording the absorbance at 652 nm on a UV-vis absorption spectrometry of the oxidation product of TMB. It should be mentioned that the absorbance changes at both 450 nm and 652 nm were measured on a UV-vis spectrophotometer for reactions in {water + TBA} mixtures.

The apparent steady-state kinetics analysis was carried out using IL-CDs (0.85 mg L^{-1}) in the citrate–phosphate buffer solution (pH 3.5, 0.2 M) at various concentrations of TMB and a series of fixed H_2O_2 concentrations at a temperature of 45 °C. The concentration of the oxidized TMB product was calculated by the Lambert–Beer law. Apparent steady-state reaction rates v at different concentrations of substrate were obtained with a typical relative uncertainty of 2% by calculating the slopes of initial concentration changes with time.

3. Results and discussion

3.1 Peroxidase-like activity and kinetic analysis of IL-CDs

The synthesized IL-CDs exhibited excellent mono-dispersed spherical structures with an average diameter of 7.1 ± 0.4 nm. The zeta potential of IL-CDs was determined to be 11 mV, which remained stable during the experimental period of 6 months with no obvious change. The UV-vis absorption spectra shown in Fig. 1b indicate a new absorption peak at 350 nm for the as-synthesized IL-CDs. The FT-IR spectrum of IL-CDs shown in Fig. 1c displays a series of peaks at 1775, 1702, 1641 and 1562 cm^{-1}, which can be assigned to the stretching vibrations of C=O in carboxyl, ketone, and amide, and bending vibrations of N–H, respectively.[15,16] Moreover, the peaks from [APMIm][Br] (such as N–H stretching vibrations at 3154 cm^{-1} and 3108 cm^{-1}, and C–N stretching vibrations at 1169 cm^{-1})[14] are present in those of IL-CDs, indicating that the surface of IL-CDs may be modified by [APMIm][Br] molecules. Besides, the X-ray diffraction (XRD) measurements show a broad peak centered at 25.3° for IL-CDs, as shown in Fig. 1d, indicating that the carbon in IL-CDs is amorphous.

The chemical composition and structure of IL-CDs were further analyzed by X-ray photoelectron spectroscopy (XPS) measurements. The XPS spectrum confirms that IL-CDs are composed of carbon, nitrogen, oxygen and bromine elements (Fig. 1e). Furthermore, the high resolution XPS spectra of C 1s, O 1s, N 1s, and Br 3d are displayed in Fig. 1f to i. Three main peaks at 284.8, 285.9 and 288.5 eV are presented in the fine structure spectra of C_{1s}, which are attributed to graphitic, nitrous and oxygenated carbon atoms, respectively.[14] The fine spectra of O_{1s} shown in Fig. 1g displays two peaks belonging to C–O and C=O.[17] The three peaks at 401.8 eV, 401.5 eV, and 398.1 eV for N_{1s} (Fig. 1h) are ascribed to C–N, N–H and C=N bonds, respectively.[14,17] Therefore, it is appropriate to speculate from the above-mentioned results that [APMIm][Br] is present on the surface of IL-CDs, which is consistent with UV-vis and FT-IR measurements.

The peroxidase-like behavior of the IL-CDs was investigated using 3,3′,5,5′-tetramethylbenzidine (TMB) as the chromogenic substrate. A series of control experiments were performed to investigate the enzymic activity of the IL-CDs, as shown in Fig. 2a. It is clearly suggested that the catalytic oxidation of TMB by H_2O_2 can only be achieved in the presence of IL-CDs.

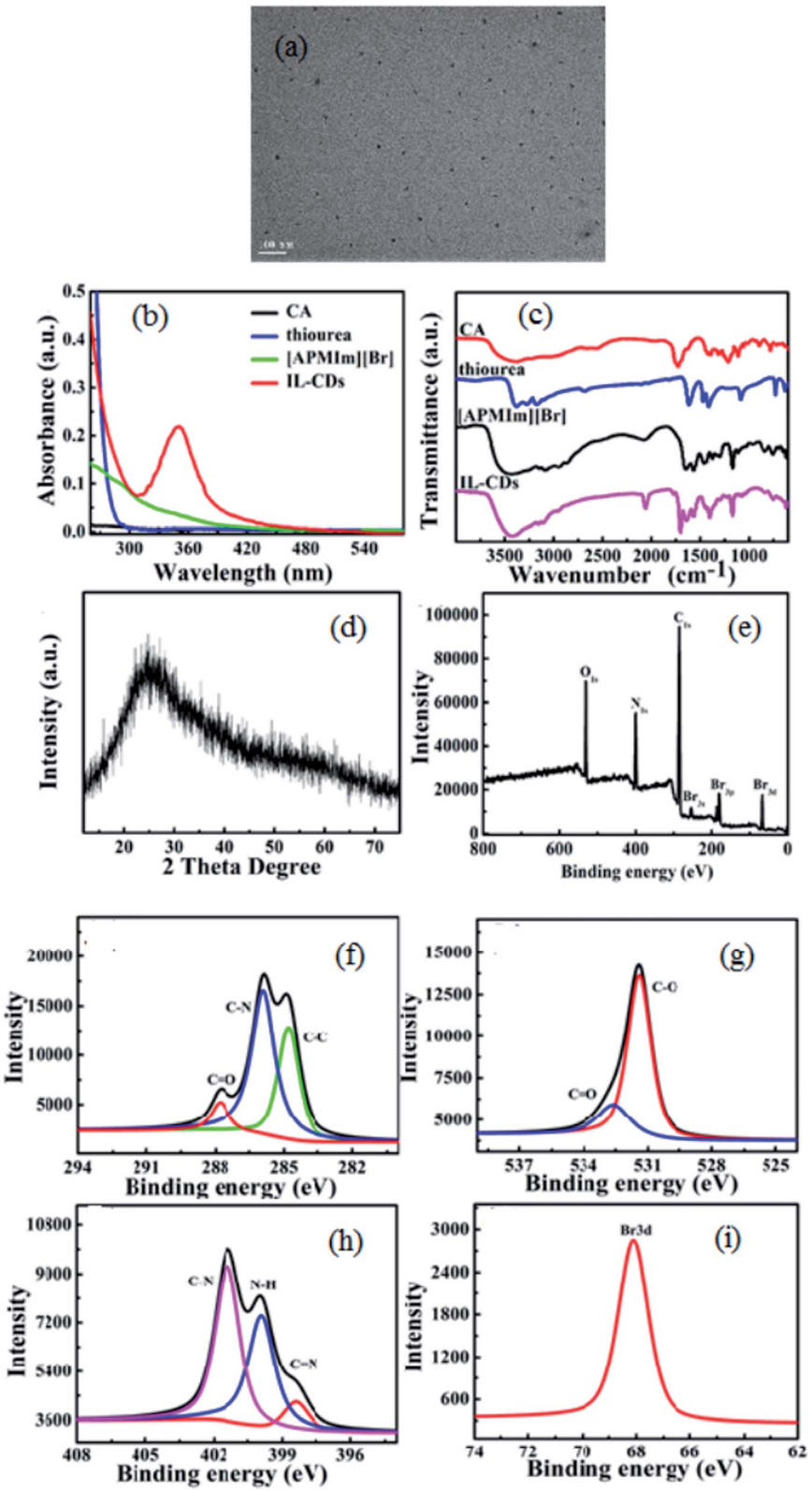

Fig. 1 (a) HRTEM image of IL-CDs; (b) UV-vis spectra and (c) FTIR spectra of CA, thiourea, [APMIm][Br] and IL-CDs; (d) XRD spectrum and (e) XPS spectrum of the IL-CDs; (f) to (i) high resolution XPS spectra of C 1s, O 1s, N 1s, and Br 3d.

We further studied the effects of pH and temperature on the catalytic activity of IL-CDs based on the relative activity A_i/A_m, where A_i is the absorbance at 652 nm for oxidized TMB (ox-TMB) at different reaction conditions and A_m is the maximum absorbance. As displayed in Fig. 2b and c, the optimal experimental conditions for the catalytic oxidation of TMB by IL-CDs

are around pH = 3.5 and T = 45 °C. Moreover, a high relative activity of 60% at 55 °C indicates good thermal stability of IL-CDs.

Under the optimal conditions (pH = 3.5 and T = 45 °C), steady-state kinetics experiments were conducted by changing the concentration of one substrate with that of the other substrate being fixed. Changes of apparent steady-state reaction rates v with TMB concentration obtained at a fixed H_2O_2 concentration (133 mM, 200 mM, 267 mM and 333 mM) are shown in Fig. 2d. The quantitative steady-state kinetic analysis by the Michaelis–Menten equation is carried out to get deep insights into the catalytic oxidation:

$$v = \frac{v_{max}[TMB][H_2O_2]}{K_m^{TMB}[H_2O_2] + K_m^{H_2O_2}[TMB] + [TMB][H_2O_2]} \quad (1)$$

where Michealis constant K_m is an indicator of the affinity of the enzyme for the substrate TMB. Lineweaver–Burk plots at a series of fixed H_2O_2 concentration are presented in Fig. 2e, where the parallel lines suggest a ping-pong mechanism for the catalytic oxidation of TMB by H_2O_2 in the presence of IL-CDs.[1] Thereafter, Fig. 2f shows the plots of the obtained intercepts (I) from Fig. 2e against the reciprocal of H_2O_2 concentration, which gives the values of K_m and v_{max} to be 0.893 mmol L^{-1} and 2.62 × 10^{-8} M s^{-1}, respectively. For the un-modified CDs, the corresponding K_m and v_{max} were 0.470 mmol L^{-1} and 4.72 × 10^{-8} M s^{-1}, respectively.[8] That is, IL-CDs were less active than the unmodified CDs due to the fact that the surface of the IL-CDs contains a large number of amino groups that would repel with the two amino groups on the surface of TMB, reducing its affinity for the substrate TMB. This is reflected by the zeta potential of CDs (0.5 mV) and IL-CDs (11 mV). However, it

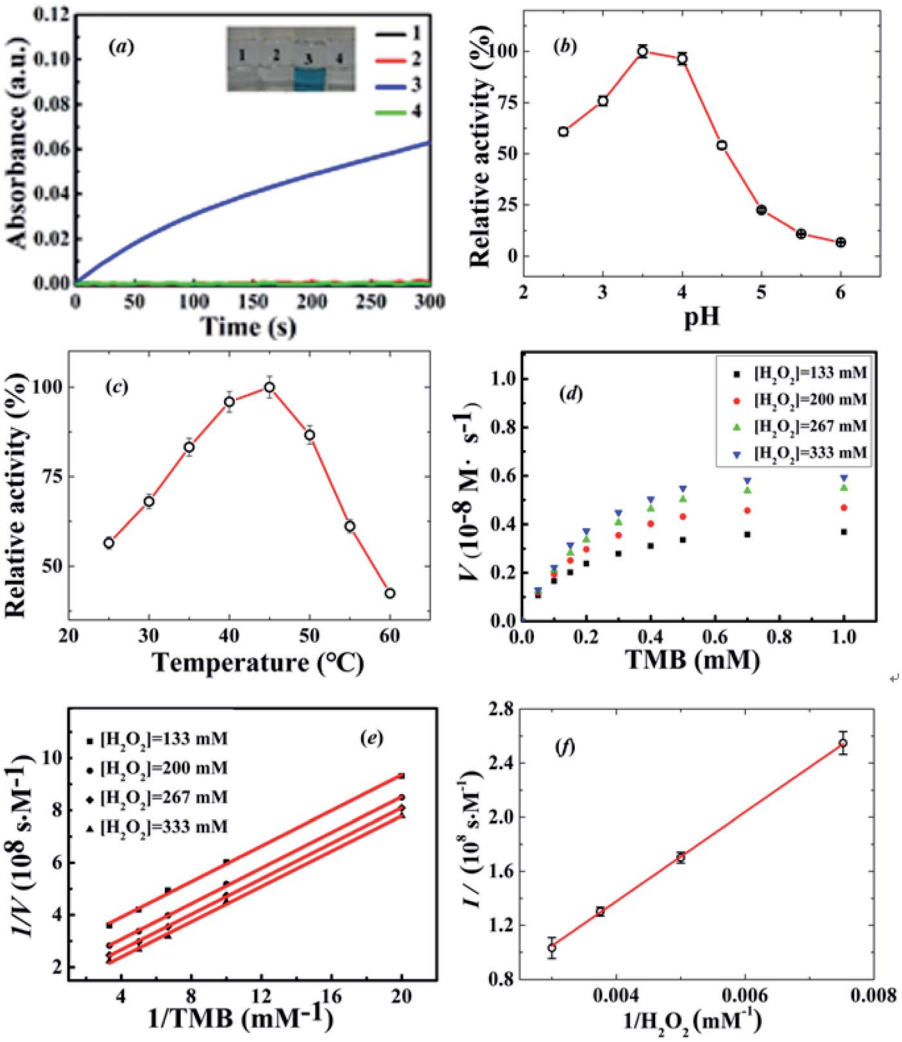

Fig. 2 (a) Time-dependent absorbance of oxidized TMB (ox-TMB) at 652 nm in different systems: (1) TMB/H_2O_2, (2) IL-CDs + H_2O_2, (3) IL-CDs + TMB + H_2O_2, (4) IL-CDs + TMB; the inset shows the photos of corresponding systems. (b) and (c) show the relative activity of IL-CDs at different pH and temperatures; (d) steady-state kinetics assay of IL-CDs with concentration of H_2O_2 being fixed at 133 mM, 200 mM, 267 mM, and 333 mM, respectively and that of TMB varied; (e) double reciprocal plots of the activity of IL-CDs with the concentration of H_2O_2 being fixed at 133 mM, 200 mM, 267 mM, and 333 mM, respectively, and that of TMB varied; (f) plot of the obtained intercepts I in (e) against the reciprocal of H_2O_2 concentration.

should be mentioned that although IL-CDs displayed a slight decline in the enzymic activity, the presence of a higher surface charge would be favorable their stability and the interaction with negative surfactants to construct new structures, which has been discussed in section 3.3.

3.2 Peroxidase-like activity of IL-CDs in hydrotrope solution

The catalytic oxidation of TMB was carried out in an aqueous solution of a well-known hydrotrope, TBA. We first investigated the reaction in pure TBA in the presence and absence of IL-CDs. It was found that TBA itself did not show enzymic activity in the catalytic oxidation of TMB. In the presence of IL-CDs, it can be seen in Fig. 3a that a yellow oxidation product with a maximal absorbance at 450 nm is presented in TBA, which may be due to the direct two-electron catalytic oxidation of TMB in organic solvents.[18] While in aqueous solutions, it is difficult to retain the equilibrium between the free cation radical from the one-electron oxidation of TMB and the charge transfer complex; thus, a blue color product is obtained.

Furthermore, the catalytic oxidation was conducted in TBA aqueous solutions at different TBA mass fractions. As shown in Fig. 3b, two oxidized products of TMB are presented, characterized by the absorbance at 450 nm and 652 nm, respectively. A plot of the ratio of the absorbance at 652 nm and 450 nm $A_{652\ nm}/A_{450\ nm}$ as a function of the mass fraction of TBA ω_{TBA} is shown in Fig. 3c, where a general decrease tendency of the $A_{652\ nm}/A_{450\ nm}$ value is observed. This may be due to that reason with the increase in ω_{TBA}, the organic solvent in the system increases and the polarity of the reaction medium decreases, leading to the occurrence of the direct double-electron catalytic oxidation of TMB to form a yellow product. However, an anomaly is clearly indicated when the mass fraction of TBA is about 0.15, where $A_{652\ nm}/A_{450\ nm}$ shows a slight increase of about 0.16. This is significantly larger than the uncertainty of $A_{652\ nm}/A_{450\ nm}$ which was estimated to be about 0.02. It has been shown that various thermodynamic properties of TBA aqueous solutions presented different extents of anomaly around the molar fraction of TBA being 0.04 (mass fraction being 0.15), which was attributed to the formation of a microscopic heterogeneous structure.[19–21] Thus, most TBA molecules may be presented in the aggregates and it is easier for the aqueous solution to retain the equilibrium between the free cation radical from the one-electron oxidation of TMB and the charge transfer complex, giving more one-electron catalytic oxidation product (blue color one with maximum absorbance wavelength at 652 nm). Therefore, $A_{652\ nm}/A_{450\ nm}$ showed a slight increase around the mass fraction of TBA being 0.15, where the aggregate concentration reached a maximum. It should be mentioned that the presence of TBA showed no obvious influence on IL-CDs, as indicated by the TEM image shown in Fig. 3d, where the mono-disperse spherical structures of IL-CDs were unchanged with a diameter being about 6–7 nm similar to that observed in the absence of TBA.

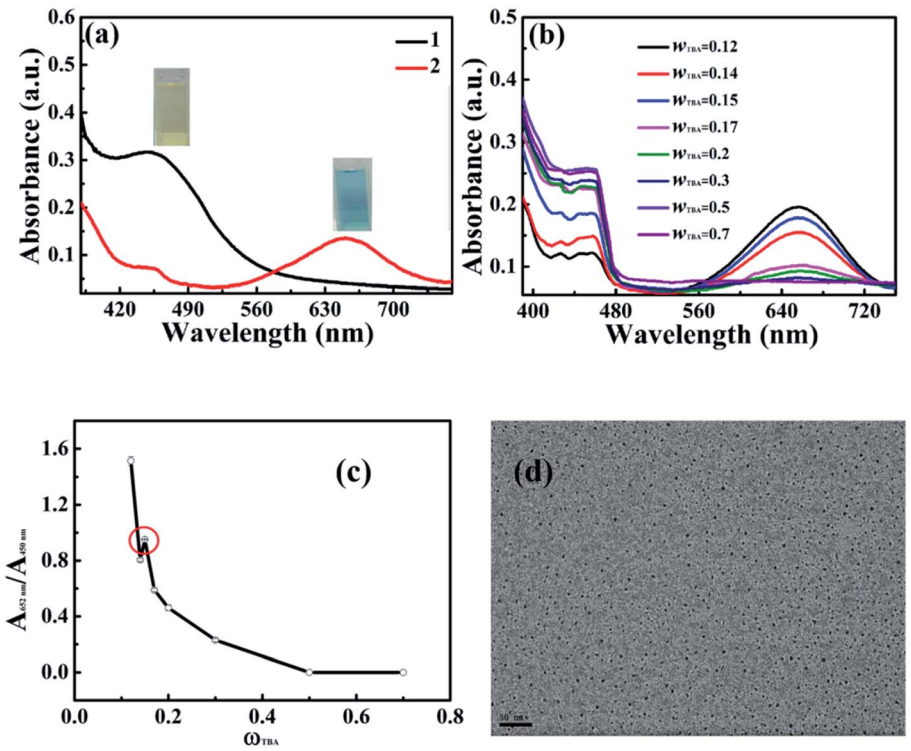

Fig. 3 (a) The UV-vis spectra of oxidized-TMB catalyzed by IL-CDs in TBA (1), and in aqueous solution (2) at a reaction time of 10 min; the inset shows the photos of the reaction systems in water (blue color) and in TBA (yellow color), respectively. (b) The UV-vis spectra of oxidized-TMB catalyzed by IL-CDs in TBA aqueous solutions with different TBA mass fractions at a reaction time of 1 hour. (c) Ratio of the absorbance of oxidized TMB at 652 nm and 450 nm, *i.e.* $A_{652\ nm}/A_{450\ nm}$, as a function of the mass fraction of TBA in aqueous solutions. (d) HRTEM image of IL-CDs in the TBA aqueous solution (mass fraction of TBA being 0.15).

3.3 Peroxidase-like activity of IL-CDs in AOT aqueous solutions

It has been shown that CDs can act as building blocks for the construction of vesicles or microemulsions together with commonly used surfactants, which may greatly enrich the application of these systems.[22,23] Therefore, we further investigated the catalytic performance of IL-CDs in the aqueous solution of a traditional anionic surfactant AOT.

The phase behavior of IL-CDs mixed with anionic surfactants AOT in water was observed with the concentration of IL-CDs being fixed at 0.5 mg mL^{-1}. As shown in Fig. 4a, the IL-CD aqueous solution gradually turns turbid with the increase in the AOT concentration and a white precipitate is presented when the concentration of AOT is about $C = 0.3$ mM. When C_{AOT} is further increased, the precipitate re-dissolved to form an opalescent solution. However, by continuously increasing the AOT concentration up to $C = 1.0$ mM, the solution became transparent again.

To get deep insights into the phase behavior, the zeta potential was measured as a function of the AOT concentration and is shown in Fig. 4b, where the zeta potential decreases with the increase in the AOT concentration. Zeta potential equals to zero when the AOT concentration is about 0.3 mM, where the aggregates formed by AOT and IL-CD precipitate. Moreover, negative staining TEM (NS-TEM) images of the mixed solution with AOT concentration being 0.1 mM and 1.0 mM AOT were obtained and are shown in Fig. 4c, which clearly suggest that vesicular structures were formed by IL-CDs and AOT with an average size of about 200 nm.

Furthermore, we studied the peroxidase-like activity of IL-CDs in different vesicular structures. As shown in Fig. 4d, it is clearly suggested that IL-CDs in the 1.0 mM AOT aqueous solution show much higher enzymatic activity towards the oxidation of TMB in the presence of H_2O_2 than those in the 0.1 mM AOT aqueous solution and in water. This may be attributed to the different vesicle structures at different AOT concentrations. When the AOT concentration is 0.1 mM, the surface of IL-CDs may partially be neutralized by AOT, which may further lead to self-assembly into AOT@IL-CD-type positively-charged vesicles. With the increase in the AOT concentration, IL-CD@AOT-type negatively charged vesicles may present. The negatively charged vesicular structure had stronger affinity towards TMB, thus showing higher enzymatic activity. The possible structures are illustrated in Fig. 4e, which are similar to the CQD/AOT mixtures reported by Li *et al.*[22]

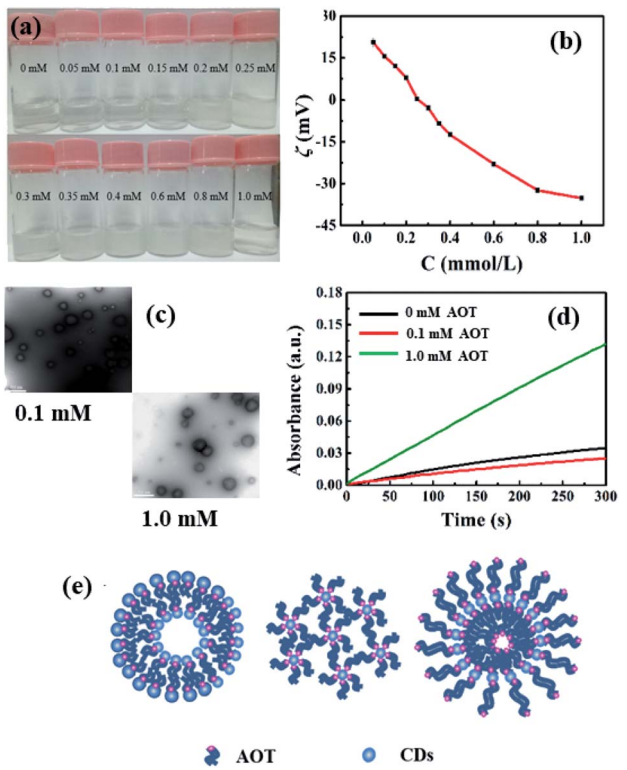

Fig. 4 (a) Photos of 12 mixed solutions of 0.5 mg ml^{-1} IL-CDs with AOT at different concentrations. (b) Variance of the zeta potential of the mixed solution of IL-CDs and AOT with the concentration of AOT. (c) NS-TEM images of the mixed solutions of IL-CDs and AOT with the concentration of AOT being 0.1 mM and 1.0 mM, respectively. (d) Time-dependent absorbance changes at 652 nm of oxidized TMB in different reaction systems with 0.5 mg ml^{-1} IL-CDs and AOT at different concentrations being 0 mM, 0.1 mM, and 1.0 mM, respectively. (e) Illustration of the possible aggregate structure at different AOT concentrations (0.1 mM, 0.3 mM, and 1.0 mM from left to right, respectively).

4. Conclusions

In summary, in this study, ionic liquid-modified carbon dots (IL-CDs) were synthesized *via* a simple method. The peroxidase-like activity of IL-CDs was explored in water and amphiphilic aqueous solutions. The catalytic activity of IL-CDs towards TMB in the presence of H_2O_2 was lower as compared to the unmodified CDs we reported previously, which can be ascribed to the positively charged surface showing poor affinity towards TMB. We further investigated the enzymic behavior of IL-CDs in two different amphiphilic molecules. In the aqueous solution of TBA, the one-electron oxidation product coexisted with the two-electron oxidation product, and the ratio of these two products decreased with the increase in the TBA mass fraction. However, when the mass fraction of TBA is around 0.15, a slight increase in the one-electron oxidation product was presented due to the formation of a microscopic heterogeneous aggregate of TBA and water molecules, which resulted in an easier equilibrium between the free cation radical from the one-electron oxidation of TMB and the charge transfer complex. When the enzymic oxidation was carried out in AOT aqueous solutions, the situation became more complicated. IL-CDs together with AOT molecules can form different types of self-assembled structures at different AOT concentrations, that is, positively-charged vesicles formed at low AOT concentrations, followed by the formation of a precipitate, and negatively-charged vesicles existed at high AOT concentrations. The variance of the vesicle structure resulted in different enzymic activities of the IL-CD/AOT complex. The results presented herein suggest that both the surface charge and the solvent environment are important factors to tune the catalytic activity of nanoenzymes.

Conflicts of interest

There are no conflicts to declare.

Acknowledgements

This work was supported by the National Natural Science Foundation of China (Projects 21773063).

References

1 L. Z. Gao, J. Zhuang, L. Nie, J. Zhang, Y. Zhang, N. Gu, T. Wang, J. Feng, D. Yang, S. Perrett and X. Y. Yan, *Nat. Nanotechnol.*, 2007, **2**, 577–583.
2 F. Attar, M. G. Shahpar, B. Rasti, M. Sharifi, A. A. Saboury, S. M. Rezayat and M. Falahati, *J. Mol. Liq.*, 2019, **278**, 130–144.
3 Y. Chong, Q. Liu and C. C. Ge, *Nano Today*, 2021, **37**, 101076.
4 X. Xu, R. Ray, Y. Gu, H. J. Ploehn, L. Gearheart, K. Raker and W. A. Scrivens, *J. Am. Chem. Soc.*, 2004, **126**, 12736–12737.
5 S. Anwar, H. Z. Ding, M. S. Xu, X. L. Hu, Z. Z. Li, J. M. Wang, L. Liu, L. Jiang, D. Wang, C. Dong, M. Q. Yan, Q. Wang and H. Bi, *ACS Appl. Bio Mater.*, 2019, **2**, 2317–2338.
6 C. C. Long, Z. X. Jiang, J. F. Shangguan, T. P. Qing, P. Zhang and B. Feng, *Chem. Eng. J.*, 2021, **406**, 126848.
7 C. Zheng, X. Q. An and T. X. Yin, *New J. Chem.*, 2017, **41**, 13365–13369.
8 J. Shi, T. X. Yin and W. G. Shen, *Colloids Surf., B*, 2019, **178**, 163–169.
9 X. Lin and X. W. Chen, *Microchim. Acta*, 2019, **186**, 1–9.
10 X. H. Wang, K. G. Qu, B. L. Xu, J. S. Ren and X. G. Qu, *Nano Res.*, 2011, **4**, 908–920.
11 Y. L. Guo, X. Y. Liu, C. D. Yang, X. D. Wang, D. Wang, A. Iqbal, W. S. Liu and W. W. Qin, *ChemCatChem*, 2015, **7**, 2467–2474.
12 T. Sela, X. X. Lin and A. Vigalok, *J. Org. Chem.*, 2017, **82**, 11609–11612.
13 S. Krickl, D. Touraud, P. Bauduin, T. Zinn and W. Kunz, *J. Colloid Interface Sci.*, 2018, **516**, 466–475.
14 B. G. Wang, A. X. Song, L. Feng, H. Ruan, H. G. Li, S. L. Dong and J. C. Hao, *ACS Appl. Mater. Interfaces*, 2015, **7**, 6919–6925.
15 J. Y. Yin, H. J. Liu, S. Z. Jiang, Y. Chen and Y. F. Yao, *ACS Macro Lett.*, 2013, **2**, 1033–1037.
16 S. Zhu, Q. Meng, L. Wang, J. Zhang, Y. Song, H. Jin, K. Zhang, H. C. Sun, H. Y. Wang and B. Yang, *Angew. Chem., Int. Ed.*, 2013, **52**, 3953–3957.
17 B. B. Campos, R. Contreras-Caceres, T. J. Bandosz, J. Jimenez-Jimenez, E. Rodriguez-Castellon, J. C. G. E. Silva and M. Algarra, *Carbon*, 2016, **106**, 171–178.
18 N. Li, Y. Yan, B. Y. Xia, J. Y. Wang and X. Wang, *Biosens. Bioelectron.*, 2014, **54**, 521–527.
19 G. Roux, D. Roberts, G. Perron and J. E. Desnoyers, *J. Solution Chem.*, 1980, **9**, 629–647.
20 Y. Koga, W. Y. U. Siu and T. Y. H. Wong, *J. Phys. Chem.*, 1990, **94**, 7700–7706.
21 K. Zemankova, J. Troncoso, C. A. Cerdeirina, L. Romani and M. A. Anisimov, *Chem. Phys.*, 2016, **472**, 36–43.
22 X. F. Sun, Q. H. Zhang, K. Y. Yin, S. J. Zhou and H. G. Li, *Chem. Commun.*, 2016, **52**, 12024–12027.
23 M. N. Hou, Q. Li, X. X. Liu, C. Lu, S. Li, Z. Z. Wang and L. P. Dang, *J. Agric. Food Chem.*, 2018, **66**, 6917–6925.